# THE INTERNATIONAL JOURNAL OF SCIENCE & TECHNOLEDGE

## Eye Detection Morphological And Magnetic Field Mapping With Digital Image Processing

**Sujoy Bhowmick**
Assistant Professor,  I.T. Department, Aryabhatta Institute Of Engineering And Management
Durgapur, W.B., India
**Himadri Nath Moulick**
Assistant Professor, C.S.E. Department, Aryabhatta Institute Of Engineering And Management
Durgapur, W.B., India
**Joyjit Patra**
Assistant Professor, C.S.E. Department, Aryabhatta Institute Of Engineering And Management
Durgapur, W.B., India

*Abstract:*
*Eye detection is required in many applications like eye-gaze tracking,iris detection, videoconferencing, auto-stereoscopic displays, face detection and face recognition. This paperproposes a novel technique for eye detection using color and morphological image processing. Itis observed that eye regions in an image are characterized by low illumination, high densityedges and high contrast as compared to other parts of the face. The method proposed is based on assumption that a frontal face image (full frontal) is available. Firstly, the skin region is detected using a color based training algorithm and six-sigma technique operated on RGB, HSV and NTSC scales. Further analysis involves morphological processing using boundary region detection and detection of light source reflection by an eye, commonly known as an eye dot. This gives a finite number of eye candidates from which noise is subsequently removed. Thistechnique is found to be highly efficient and accurate for detecting eyes in frontal face images.Optical position measurement system for an automated magnetic field mapping apparatus based on fluxgate sensors is presented. For the exact position estimation of the sensor head, a simple smart camera wasdeveloped with respect to minimal hardware configuration and real-time execution of position measurement algorithm. The camera is observing the mapped scene and evaluates position of the sensor head using an activemarker. The sensor head is designed as movable, what allows keeping the scene fixed and exactly referenced tothe mapped magnetic field using coordinates obtained from image. With image sensor fixed 2.5 m above the planeand range ±130 mm around the lens optical axis (image center), the total position measurement error is less than 0.5 mm.*

*Key words: Position measurement, smart camera, magnetic field mapping*

## 1.Introduction

Human face image analysis, detection and recognition have become some of the mostimportant research topics in the field of computer vision and pattern classification. The potential applications involve topics such as face detection, face identification and recognition, and facial expression analysis. Among these research topics, one fundamental but very important problem to be solved is automatic eye detection. The eye is the most significant and important feature in a human face, as extraction of the eyes are often easier as compared to other facial features. Eye detection is also used in person identification by iris matching. Only those image regions that contain possible eye pairs will be fed into a subsequent face verification system. Localization of eyes is also a necessary step for many face classification methods. For comparing two faces, the faces must be aligned. As both the locations of eyes and the inter-ocular distance between them are relatively constant for most people, the eyes are often used for face image normalization. Eye localization also further facilitates the detection of other facial landmarks. In addition, eyes can be used for crucial face expression analysis for human computer interactions as they often reflects a person's emotions.The commonly used approaches for passive eye detection include the template matching method [6, 7], eigenspace [2, 3, 8] method,and Hough transform-based method [1, 4]. In the template matching method, segmentsof an input image are compared to previously stored images, to evaluate the similarity of the counterpart using correlation values. The problem with simple template matching is that it cannot deal with eye variations in scale, expression, rotation and illumination. Use of multiscale templates was somewhat helpful in solving the previous problem in template matching. A method of using deformable templates is proposed by Yuille et al [9]. This provides the advantage of finding some extra features of an eye like its shape and size at the same time. But the rate of success of this approach depends on initial position of the template. Pentland et al. [8] proposed an eigenspace method for eye and face detection. If the training database is variable with respect to appearance, orientation, and illumination, then this method provides better performance than simple template matching. But the performance of this method is closely related to the training set used and this method also requires normalized sets of training and test images with respect to size and orientation.

Another popular eye detection method is obtained by using the Hough transform. This method is based on the shape feature of an iris and is often used for binary valley or edge maps [10, 11]. The drawback of this approach is that the performance depends on threshold values used for binary conversion of the valleys. Apart from these three classical approaches, recently many other image-based eyedetection techniques have been reported. Feng and Yuen [12] used intensity, the direction of the line joining the centers of the eyes, the response of convolving an eye variance filter with the face image, and the variance projection function (VPF) [13] technique to detect eyes. Zhou and Geng [14] extended the idea of VPF to the generalized projection function (GPF) and showed with experimental results that the hybrid projection function (HPF), a special case of GPF, is better than VPF and integralprojection function (IPF) for eye detection.Kawaguchi and Rizon [10] located the irisusing intensity and edge information. They used a feature template, a separability filter,the Hough transform, and template matching in their algorithm. Sirohey and Rosenfeld [24] proposed an eye detection algorithm based on linear and nonlinear filters. Huang and Wechsler's method [16], used genetic algorithms and built decision trees to detect eyes. For the purpose of face detection, Wu and Zhou [17] employed size and intensity information to find eye-analog segments from a gray scale image, and exploited thespecial geometrical relationship to filter out the possible eye-analog pairs. Han et al. [18]applied such techniques as morphological closing, conditional dilation and a labelingprocess to detect eye-analog segments. Hsu et al. [19] used color information for eyedetection.Although much effort has been spent and some progress has been made, the problemof automatic eye detection is still far from being fully solved owing to its complexity.Factors including facial expression, face rotation in plane and depth, occlusion andlighting conditions, all undoubtedly affect the performance of eye detection algorithms.The method proposed in this paper involves skin detection to eliminate background components followed by eye detection. In the field of magnetic measurements one of frequent tasks is to measure magnetic field distribution – magnetic field mapping. Field mapping is used for example for ferromagnetic markers detection in biomedical diagnostics. One of possible methods for mapping of magnetic field is to use a movable sensor head which is moved along the scanned area [1]. Position of the head and measured value are processed to obtain a 2D magnetic field map. A crucial task that influences the overall mapping spatial resolution is position estimation of the moving head. If DC magnetic fields in order of 10-9 T are to be measured, it is necessary to ensure that the measured magnetic field is not affected by the measurement method or the used instrument (by construction parts of the position sensor). Thus the position measurement has to be based on a contactless method that allows the position sensor to be placed in an adequate distance not affecting the measured field by its construction parts (e.g. metal components). A reasonable solution is to use an optical principle for position measurement, which allows using even non-perfect positioning stage with a non-magnetic sensor arm, avoiding the need for expensive, non-magnetic positioning systems, which are also limited in service-life. For high precision position measurement a laser-interferometer can be used. Spatial resolution of a multi-dimensional position measurement system [2] is about 0.07 mm in wide-range, but construction severity and price are very high. For the task of magnetic field mapping, about 1 mm spatial resolution of the measurement head position is satisfactory (in the range of 700mm x 700 mm). Thus position measurement based on digital image processing is reasonable allowing for lower complexity and costs.With the growing performance of computational tools, image-based measurement systems are frequently used instead of conventional sensors (sets of sensors) for measurements of physical quantities (measured quantity has to be convertible to visually observable form). Generally image-based sensors can be constructed as PC-based Systems (image information is acquired by an externalcamera connected to a PC using a frame-grabber, image is processed in the PC), Stand-alone Image Processing Units (external camera is connected to a stand-alone processing unit whose performance is optimized for image processing algorithms) or Smart Cameras (devices which are embedding image acquisition and processing into a single device). The basic advantage of the last mentioned sensors is their compactness and portability, providing still adequate computational performance for less demanding algorithms. Complexity of the algorithm can be decreased using a-priori information that simplifies image processing. For the position measurement task such simplification can be a well-defined object (marker), fixed to the object whose position is evaluated. If this object has significant and unique brightness profile it is very simple to recognize it in the observed scene and calculate its position. For the real world measurements objects of interest are usually not easy recognizable, but in many tasks an external marker can be added to highlight the measured object. This approach when extra information is added into the image of the measured object to simplify the image processing is called Assisted Videometry. In our case of the magnetic field mapping apparatus a Light Emitting Diode (LED) is fixed on the movable sensor head and serves as an active marker simplifying image processing. Less demands on image-processing performance allowed us to choose a smart camera variant as appropriate for our purpose, adding portability of the position sensor.

**2.Skin Detection**
The detection of the skin region is very important in eye detection. The skin region helps determining the approximate eye position and eliminates a large number of false eye candidates. In this paper, we have
used a combination of HSV, RGB and NTSC spaces to increase the efficiency of eye detection. The following training techniques were used for detection. First, the code was trained manually on a few images for skin color. The data was obtained for all the color space components, and was fitted to a Gaussian curve. Care must be observed while training, to avoid unwanted pixels like facial hair and creases, as we trained images for only one peak and that peak should be the color of skin. Finally, the six-sigma technique was used for detection. It was observed that HSV space was the most efficient space for skin detection. Figure 2 represents the skin detected region from figure 1.
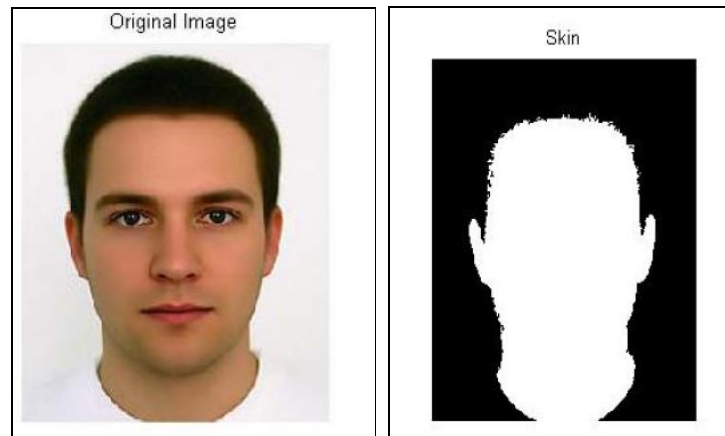
*Figure 1: Original Image & Figure 2: Skin Detection*

### 3.Eye Detection

The eye detection technique used here is based on the fact that whenever an eye is properly illuminated, it has a sharp point of reflection. This point will be referred to as alight dot. NTSC format is most efficient in exploiting this light dot. Hence, the image is first converted into an NTSC image and the chrominance values of its pixels are used for further processing. The next step in eye detection involves edge detection. Morphological techniques are used for boundary detection. Dilation, followed by erosion and the calculation of differences between the two produces an image with boundaries. The structuring element used in dilation and erosion has a large matrix ($9\times9$ ones), so that clear and thick boundaries are detected. For the purpose at hand, this technique is found to be more efficient that the Canny edge detector. This is followed by suitable thresholding of the image. The light dot is one of the first few candidates that stand out when the image is thresholded. Selection of a proper thresholding value is important, and a complex process, as this value varies as the image changes. Hence, an adaptive thresholding technique is used. Calculation of this value is achieved by an iteration process. The value is started at 220 on a 255 scale and is decreased by 5 per iteration. The aim of the iteration process is to obtain a minimum number of four and a maximum number of six blobs. It was observed statistically that between these values, thresholding is most probable to output both eyes and with minimum noise. Thresholding is followed by morphological closing, which improves the ease of eye detection and eliminates stray points. Sample outputs of figure 3 are shown in figure 4. Some of the blobs obtained in the image are too small, and some are too large, and both are unlikely to be candidates for an eye. Hence, they are morphologically eliminated. This is followed by eliminating long and slender blobs, either horizontal or vertical ones, as these blobs are certainly not eyes. Again, morphological binary image processing is used. This image and skin image are combined by using an 'And' operation. Only the common candidates survive, as eyes invariably lie in the face region. This whole process is included in a loop and the number of emerging candidates is checked at the end of the loop. If this number is not between 4 and 6, the threshold value is changed, for the next loop
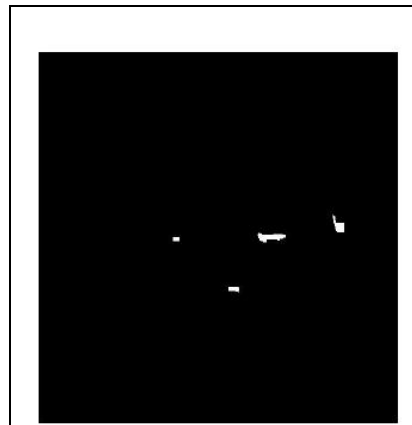


*Figure 3: Sample Result*

Now, the job at hand is to eliminate the noise and obtain the two blobs which represent the eye region. The logic used here is that in a frontal face photograph, eyes lie more or less in the same horizontal line. Hence, a condition is imposed that for a blob A, if there is no blob B, such that maximum y value of A is greater than minimum y value of B, and maximum y value of B is greater than minimum y value of A, then A is not a candidate for eye. Another condition imposed is on the lower limit and upper limit of the distance between A and B. This eliminates a considerable number of noise points. The main problem now is the condition where there are 3 points in a line. Many times, it is observed that 2 of the three points are very close to each other, and both are actually part of the same eye. This problem is tackled by horizontal dilation, which connects the two points and leaves us with two candidates, which are eyes. Figure 6 shows noise eliminated image from figure 5.
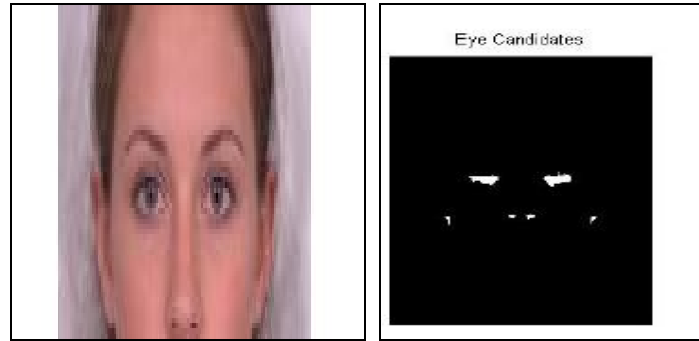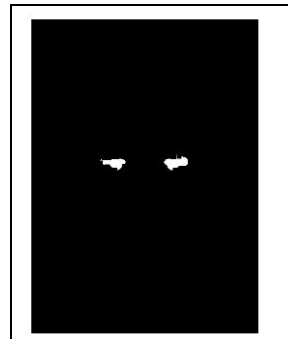
*Figure 4 & Figure 5: Eye Candidates*



*Figure 6: Detected Eye Regions*

**4.Smart Camera As A Position Sensor**

Optical referencing of the sensor arm position is solved by use of a simple smart camera designed for an

embedded implementation of image processing algorithms (contact-less optical measurement evaluation).

As a computational core of the smart camera usually the Field Programmable Gate Array (FPGA), digital signal processor or combination of both technologies can be used. Solutions based on the FPGA may have a high image processing performance, but reconfiguration of those systems is a time-consuming task [5]. The published DSP-based smart camera conceptions are usually equipped with a slow communication interface with the PC (comfortless due to the slow transfer rate of image data to the PC) or are lacking hardware synchronization of the measurement, which is important for data post-processing [6]. The real-time position measurement, with a-priori information in form of a marker (a point light source - LED) was implemented in a minimalistic concept of a simple smart camera based on DSP as introduced below.

**5.DSP-Based Smart Camera Conception**

Considering the mentioned real-time performance requirements and image source of CMOS technology with the direct digital interface, ADSP-BF532 Blackfin® digital signal processor was selected as a reasonable solution core. Blackfin® processor is equipped with the integrated Parallel Peripheral Interface (PPI) that in cooperation with the dedicated Direct Memory Access (DMA) channel provides a glue-less interface to the CMOS image sensor. Using this feature, almost all processor time can be effectively used for image processing (processor doesn't need to control transfer of image data from the image sensor, it is done in the background).The hardware of the smart camera is equipped with an additional 1 MB of data SRAM and a USB Full Speed driver chip for communication with PC. For synchronization of measurements a set of optically isolated inputs and outputs is available. Interface to the measurement chain is also provided by a RS-485 interface. The smart camera block diagram is depicted in Figure 7.
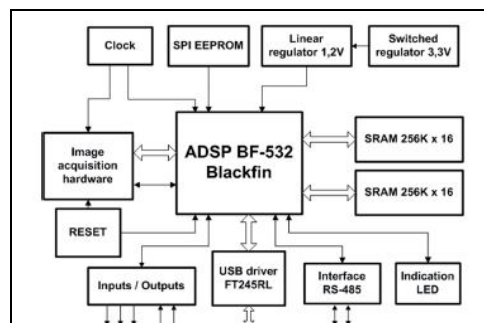


*Figure 7: The Designed Smart Camera Block Diagram*

CMOS image sensor LM9638 was used for image acquisition. Physical resolution of this image sensor is 1312x1032 pixels. Effective resolution of this image sensor is 1288 x 1032 pixels (the difference between the full physical resolution and the effective resolution is given by a group of shadowed pixels that are used for sensor calibration and image corrections). For the purpose of our measurement where the position resolution about 1 mm was required, we used a window of standard resolution of 1280x1024 pixels, which was reduced to 640x512 pixels by down-sampling using an on-chip 2x2 pixel-averaging function (binning). Decreasing of the image resolution proportionally reduced also the execution time of implemented algorithms (described below). Physical dimensions of the active photosensitive area are 7.68 x 6.144 mm with the virtual pixel size (after down sampling) 12 μm (square pixel).

### 6. Smart Camera Optical Front-End

The smart camera was equipped with a lens with fixed focal length of 25 mm (Carl Zeiss, Tevidon 1.8/25). Lens quality is strongly affecting the final measurement nonlinearity due to geometrical errors which are distorting the acquired image. A color filter was mounted on the lens for highlighting of the optical marker and suppressing the background scene (the marker and the filter were of the same color). Optical front-end and marker projection on the image sensor is depicted in Figure 8. Equation (1) describes the relationship between the horizontal field of view VH and distance d between the measured plane and the camera lens principal point. In this equation f stands for the lens focal length and SH denotes the horizontal size of the photosensitive area of the image sensor. The relation is calculated for a 25 mm lens and the image sensor with above the described parameters.

$$V_H = \frac{d-f}{f} \cdot S_H = \frac{d - 25 \cdot 10^{-3}}{25 \cdot 10^{-3}} \cdot 7.68 \cdot 10^{-3} \ [m,m]$$ ………(1)

By exchange of parameter SH with SV (vertical size of the photosensitive area) equation (1) calculates vertical field of view VV of the smart camera. View area can be also represented

by the diagonal angle of view
$$\omega = 2 \cdot arctg\left(\frac{\sqrt{S_H^{\,2} + S_V^{\,2}}}{2 \cdot \left(f + \frac{f^2}{d-f}\right)}\right) \cdot$$ ………..(2)
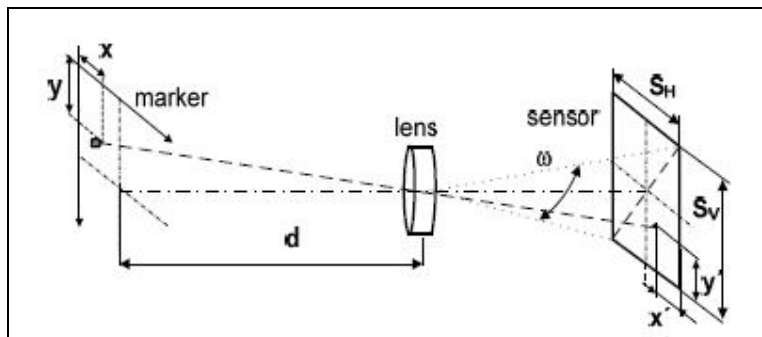


*Figure 8: Smart Camera Optical Front-End And Marker Projection*

(distances are not depicted in real ratios). Position of the object projected on the image sensor is evaluated in pixels. For calculation into real-world units equation (3) is used

$$k = \frac{f}{(d-f).S_P} = \frac{25.10^{-3}}{(d - 25.10^{-3}).12.10^{-6}} \ [pixel/m] \cdot$$ ………..(3)

In (3) k stands for calibration constant (pixel/m) and SP denotes pixel size.

### 7. Image Processing Algorithm

The principle of position estimation is based on the evaluation of active marker position – its brightness profile is depicted in Figure 9. However the LED supply current is a source of an additional magnetic field that can interact with the mapped field and

thus increase magnetic field measurement error. Therefore the LED is controlled by smart camera output and it is activated only during the time of image acquisition which is different from acquisition of the magnetic data. Another possible solution would be an optical fiber, or a retro-reflexive material with an external light source could be used on the position of the active marker (in both cases the real light or illumination source must be placed in the distance where it is not affecting the measured magnetic field). The estimated position of the active marker is calculated as a position of the group of image pixels with the highest intensities.
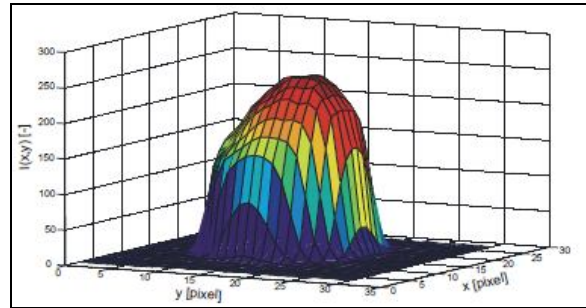


*Figure 9: Spatial Profile Of LED Brightness (Lens Aperture Set To Avoid Image Saturation).*

Assuming only one marker, significantly brighter than its background, a center of image gravity formula derived from a 2D object barycenter calculation can be used for its position estimation [7]. Its discretized form for grayscale image (4) is proper for real-time implementation with digital signal processor

$$T_x = \frac{\sum_{y=0}^{H-1} \sum_{x=0}^{W-1} x I(x,y)}{\sum_{y=0}^{H-1} \sum_{x=0}^{W-1} I(x,y)} , \quad T_y = \frac{\sum_{y=0}^{H-1} \sum_{x=0}^{W-1} y I(x,y)}{\sum_{y=0}^{H-1} \sum_{x=0}^{W-1} I(x,y)} \qquad \ldots\ldots\ldots (4)$$

In the previous equation $T_x$ and $T_y$ denote coordinates of the gravity center, $I(x,y)$ stands for image intensity value at the given point, x and y represent current coordinates in the processed image of width W and height H (in pixels). To ensure that only the pixels of the light source will be used in the calculation and the rest of the acquired image will be suppressed, the image is preprocessed using a grayscale threshold function. Pixels with intensities below the selected level are suppressed (their intensity value is calculated as 0) [8]. Due to the integral character of the calculation, resolution of obtained results is always higher than the smallest picture element (sub-pixel resolution). This feature is advantageous as no additional input data interpolation is needed and calculation provides sub-pixel results by itself. Position measurement dynamics increases abreast with the constant computation performance (for higher precision of measurement result no additional processor time is needed).

### 8.Magnetic Field Mapping System Setup
The motivation for the development of the smartcamera based positioning system was an improvement of
the existing magnetic field-mapping system. Generally, there are two concepts of automated positioning when mapping magnetic fields – holding the sensor (array) fixed and moving the scene, or vice versa. The first option is more robust and does not suffer from non-homogeneity of the background magnetic field, however, it is limited in the size of the moved object. This approach was used in mapping of the field gradient in magnetopneumography [4], where moving of the whole human body on a non-magnetic bed makes the measurement time-consuming and inefficient. However a movable sensor head offers more flexibility and is popular in commercial solutions, as moving the sensor head is usually less complex and allows easy fitting to the measured object [1]. Because the magnetic cleanliness of commercially positioning systems is often questionable we used our positioning device made from a rebuiltXY-recorder, with steel parts removed and replaced, in order to keep intrinsic magnetic moment to minimum. The movable sensor head was placed on an 80 cm long non-magnetic arm and allowed a 40 x 40 cm scene to be positioned on. On the sensor arm, a LED diode (as an active marker) was placed near the sensor head, forming the reference point to the coordinates as obtained from the smart-camera. The 5 mm shift between the marker and the center of the fluxgate sensors was numerically corrected in all the measurements. The developed position sensor was mounted 2.5 m above the measured object (Figure 10).
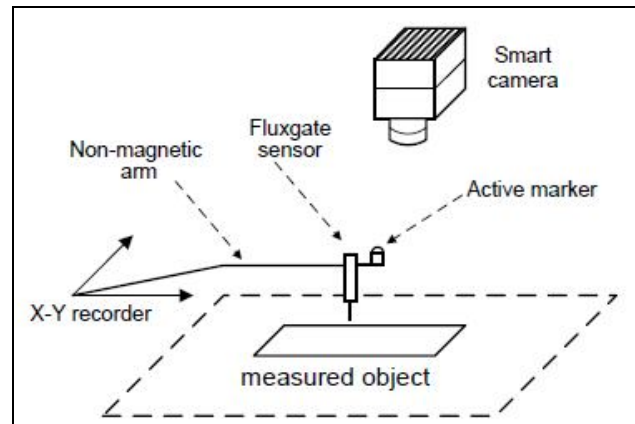
*Figure 10: Magnetic field mapping system setup*

As a magnetic field sensor, flat printed-circuit-board (PCB) fluxgate sensors of our own design were used, as they can be easily fixed in orthogonal or gradiometric setup and are sensitive enough to detect magnetic fields in nT range [10]. The sensor dimensions are 33.5 x 15.5 x 0.9 mm3, the low thickness allowed to mount the sensors forming a first order dBx/dy gradiometer with very small gradiometric base (1 mm were used) sensor distance. The sensors were operated in the 2nd harmonic mode,without any feedback loop, and the output voltage from the lock-in amplifier SR-830 (either in A or A-B mode in gradiometric setup) was fed to the acquisition system consisting of 2 HP 34401 multimeters in 6.5 digits resolution. Together with a programmable DC-current source, which generated voltages for X and Y inputs of the XYrecorder, the setup was automatically driven with LabView software which was linked to the smart-camera based position sensor with a USB interface providing coordinates reference for the positioning and data-acquisition.

### 9.Improved Magnetic Filed Mapping - Results

For evaluation of the designed setup, we visualized the remanent magnetic field of a PCB board, containing magnetometer's analog electronics used on the Czech scientific satellite Mimosa [10]. As the board was placed perpendicular to the normal component of Earth's field, which is almost 80% in our region, we could map the influence of magnetically hard and soft components magnetized by that field. We placed the sensor arm 15 mm above the PCB, the mapped normal component (after subtracting the offset due to Earth's magnetic field) is shown in Figure 7 – 1V corresponds to approx. 0.5 μT, which is 1/10 of Earth's field value and can be already in the level of environmental noise. The usability of the smart camera position sensor is not only in the overlay of measured data and the scene, but it also ensures orthogonal grid, either by the used feedback-loop, where the positioning device is referenced to the camera position readings, or by the means of post-processing in Matlab. As the measured area was still affected by the local magnetic field inhomogeneity, we decided to use the gradiometric setup as described above, with the result shown in Figure 11. The measurement step was refined to 2 mm and we were able to clearly identify a magnetic screw in the D-SUB connector, a foil capacitor and an EEPROM as main magnetically disturbing parts.
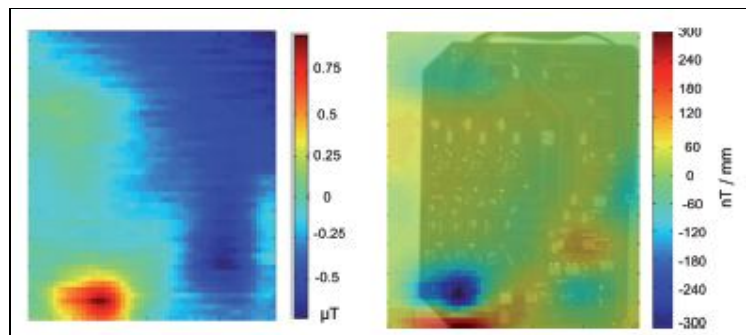


*Figure 11: Mapped Normal Field (Left) And Gradient (Right) Distribution 15mm Above The Plane*

With the help of gradiometric reading, we succeeded in mapping of the remanent field of a 1-USD banknote at 5 mm height, without any external field excitation (early results were presented in [11] but did not allow to map the data precisely without the use of position sensor). The obtained image could be transformed and fitted to the camera image, resulting in Figure 12. The depicted magnetic gradient is less than 20 nT/mm and thus the system with a contactless smart-camera based optical position sensor has proven feasible for sensitive DC magnetic field mapping in real unshielded environment.

*Figure 12:  Mapped Gradient Field Of A 1-USD Banknote, As Measured 5 Mm Above The Plane*

### 10. Conclusion And Future Work

In this paper a simple and efficient eye detection method for detecting faces in color images is proposed. It is based on a robust skin region detector which provides face candidates. This is followed by morphological processing and noise elimination which produces eye candidates. The final two candidates are selected by applying rules that define the structure of a human face. It is observed from the results that this technique is successful for 90% of frontal face images, which show two clearly illuminated eyes. However, this technique does not work for most profile images. The method also fails when one or both eyes are closed. The current code is written in MATLAB and requires 15-20 seconds of run-time on a 2GHz processor. However, it is expected that C-based code will take less than 1 second. Future work includes converting this code into the C language and to use a webcam. The webcam eye detection can be very useful and user friendly, as user can give inputs to the computer using eye movement. For example, cursor movement using gaze detection and tracking can eliminate the need for a computer mouse and can convey simplicity and userfriendliness in the operating system. Further improvement also includes detection of eyes in multiple faces, and faces with different orientations. We have developed an optical position measurement sensor based on image information processing. The sensor was designed as the stand-alone device based on digital signal processor Blackfin® and CMOS image sensor. Basic motivation for the sensor development was improvement of a method for 2D magnetic field mapping by increasing its spatial resolution. Although the required and fully satisfactory position  resolution was about 1 mm, the total position measurement error of the developed sensor was less than 0.5 mm which results non-linearity about 0.2 % of the full–scale. In the area very close to the optical center ($\pm$ 30 mm) this nonlinearitywas less than 0.1%. Position measurement uncertainty can be decreased by averaging of measured values. With the use of the developed camera as a position sensor for the magnetic field mapping system, the measured magnetic field distribution can be directly mapped into the acquired image of the mapped object and thus improve results interpretation (e.g. for field mapping in medicine).

### 11. References

1) A Robust Eye Detection Method Using Combined Binary Edge and Intensity Information. Jiatao Song, Zheru Chi, Jilin Liu. Science Direct, Pattern Recognition 39 (2006) 1110-1125.
2) A Simple and Efficient Eye Detection Method in Color Images. D.Sidibe, P.Montesinos, S.Janaqi. Parc Scientifique G.Besse, France.
3) A Hybrid Method for Eye Detection in Facial Images. Muhammed Shafi, Paul W.H.Chung.Waset. www.waset.org.
4) Digital Image Processing. R.C. Gonzalez and R.E.Woods, 2nd edition PHI, Chapter 9, Morphological Image Processing.
5) Handbook of Image and Video Processing. (AL Bovik) Section III, Chapter 3.3, Morphological Filtering for Image Enhancement and Detection.
6) R.Brunelli, T.Poggio, Face Recognition,Features versus templates, IEEE Trans.Patt. Anal. Mach. Intell. 15(10)(1993) 1042-1052.
7) D.J.Beymer, Face Recognition under varying pose, IEEE Proceedings of Int. Conference on Computer Vision and Pattern Recognition (CVPR'94), Seattle, Washington, USA,1994, pp.756-761.
8) A.Pentland, B.Mognanddam, T.Starner, View based and modular eigenspaces for face recognition in , IEEE Proceedings of Int. Conference on Computer Vision and Pattern Recognition (CVPR'94), Seattle, Washington, USA,1994, pp.756-761.
9) A.L.Yuille, P.W.Hallinan, D.S.Cohen, Feature Extraction From Faces Using Deformable Template, Int. J.Comput.Vision 8(2)(1992) 99-111.
10) K.M.Lam, H.Yan, Locating and extracting eye in human face images, Pattern Recognition, 29(5)(1996) 771-779.
11) G.Chow, X.Li, Towards a system of automatic facial feature detection, Pattern Recognition (26)(1993) 1739-1755.
12) G.C.Fang, P.C.Yuen, Multi cues eye detection on gray intensity image, Pattern Recognition (34)(2001) 1033-1046.
13) G.C.Fang, P.C.Yuen, Variance Projection function and its application to detection for human face recognition, Pattern Recognition Lett. 19(1998) 899-906.
14) Z.H.Zhou, X.Geng, Projection functions for eye detection, Pattern Recognition (37)(5)(2004) 1049-1056.
15) S.A.Sirohey, A.Rosenfield, Eye detection in a face image using linear and non linear filters, Pattern Recognition (34)(2001)(1367-1391).
16) J.Huang , H.Wechsler, Visual routines for eye localization using learning and evolution. IEEE Trans.Evol.Comput.(4)(1)(2000) 73-82.
17) J.Wu, Z.H.Zhou, Efficient face candidate selector for face detection, Pattern Recognition (36)(2003) 1175-1186.

18) CC.Hen, H.Y.M.Liao, G.J.Yu, L.H.Chen, Fast face detection via morphology based pre processing. Pattern Recognition 33(2000)1701-1712.
19) R.L.Hsu, M.Abdel Mottaleb, A.K.Jain, Face detection in color images, IEEE Trans. Patt. Anal. Mach. Intell. 24(1)(2002) 34-58.
20) TUMANSKI, S., LISZKA, A. The methods and devices for scanning of magnetic fields. Journal of Magnetic Materials, 2002, vol. 242-245, Part 2, p. 1253-1256.
21) YONGBING, L., GUOXIONG, Z. The optimal arrangement of four laser tracking interferometers in 3D coordinate measuring system based on multi-lateration. In IEEE International Symposium on Virtual Environments, Human-Computer Interfaces and Measurement Systems 2003. VECIMS '03. 2003, p. 138- 143, doi: 10.1109/VECIMS.2003.1227044.
22) El GAMAL, A., ELTOUKHY, H. CMOS image sensors. IEEE Circuits and Devices Magazine, May-June 2005, vol. 21, no. 3, p. 6- 20, doi:10.1109/MCD.2005.1438751
23) TOMEK, J., PLATIL, A., RIPKA, P., KASPAR, P. Application of fluxgate gradiometer in magnetopneumography. Sensors and Actuators A: Physical, 2006, vol. 132, no 1, p. 214-217.
24) LEESER, M., MILLER, S., YU, H. Smart camera based on reconfigurable hardware enables diverse real-time applications. In Proceedings of the 12th Annual IEEE Symposium on Field- Programmable Custom Computing Machines, 2004. IEEE Computer Society, Washington DC, p. 147-155.
25) LOVVEL-SMITH, C. D., BONES, J. P., HAYES, M. P., JOHNSTON, R.A., PRICE, N. B. 'Black Spot': A prototype camera module. In Proceedings of the 23rd International Conference on Image and Vision Computing. New Zealand, 2008, p.1-6, doi: 10.1109/IVCNZ.2008.4762112M
26) SHORTIS, R., CLARKE, T. A., SHORT, T. A comparison of some techniques for the subpixel location of discrete target images. Videometrics III, SPIE vol. 2350. Boston. p. 239-250.
27) FISCHER, J., ODLOZIL, P. FPGA based system for the measurement of a laser spot position. In Proceedings of Eurosensors XVI. Prague, 2002, p. 201-202, ISBN 80-01-02576-4
28) EGMONTON-PETERSEN, M., REIBER, J. H. C. Accurate object localization in gray level images using the center of gravity measure: Accuracy versus precision. IEEE Transactions on Image Processing, 2002, vol 11, no. 12, p 1379 - 1384, doi: 10.1109/TIP.2002.806250
29) JANOSEK, M., RIPKA, P. PCB sensors in fluxgate magnetometer with controlled excitation. Sensors and Actuators A: Physical, April 2009, vol. 151, no. 2, p. 141-144, ISSN 0924-4247, doi: 10.1016/j.sna.2009.02.002
30) JANOSEK, M., RIPKA, P., PLATIL, A. Magnetic markers detection using PCB fluxgate array. Journal of Applied Physics, 2009, vol. 105, no. 7, p. 7E717. ISSN 0021-8979.